EDSU Journal of Engineering and Technology (EDSUJET) Vol. 2 (1), pp. 137 – 149. 2026
ISSN (Print):3121 – 8725 eISSN (Online): 3121 – 8597

EDSU Journal of Engineering and Technology (EDSUJET)

Unconfined Compressive Strength Modelling of Soil Stabilized with Millet Husk Ash, Quarry Dust and Bush Gravel

Anavberokhai Isah Osigbhemhe[1] and John Wasiu[2]

[1] Department of Civil Engineering, Auchi Polytechnic, Edo State, Nigeria
[2] Department of Civil Engineering, Edo State University Iyamoh, Edo State, Nigeria
*Corresponding Author Email:** isahsworld2018@gmail.com

Received: 20 October 2025, Accepted: 2 December, 2025 Published: 31 March, 2026

KEYWORDS

Soil Stabilization
Millet Husk Ash
Bush Gravel
Quarry Dust
Microstructural analysis
Predictive Modelling

ABSTRACT

Clay soils rich in aluminosilicate minerals are often characterized by low shear strength, high plasticity, and inadequate load-bearing capacity, rendering them unsuitable for pavement and structural applications in their natural state. This research explores the stabilization of weak clay soil through the combined use of millet husk ash (MHA), quarry dust (QD), and bush gravel (BG), employing laboratory geotechnical testing, SEM–EDX microstructural characterization, and predictive modelling of unconfined compressive strength (UCS). Experimental results indicate that an optimal mixture comprising 5% MHA, 15% QD, and 25% BG increased the UCS from 289 kPa in untreated soil to 1459 kPa, representing a 405% improvement. Correspondingly, the California Bearing Ratio (CBR) rose from 4.2% to 13.2%, and maximum dry density (MDD) improved from 1.62 g/cm³ to 1.74 g/cm³. SEM–EDX analysis revealed the development of calcium–silicate–hydrate (C–S–H) gels and enhanced particle interlock as the primary mechanisms responsible for strength enhancement. Predictive modelling using Linear Regression, Gaussian Process Regression (GPR), Support Vector Regression (SVR), and Bayesian Ridge Regression demonstrated limited generalization due to the small dataset; however, GPR achieved the lowest prediction errors (MAE = 209.24 kPa, RMSE = 295.76 kPa) while allowing uncertainty quantification. The study highlights the synergistic effect of chemical and physical stabilization, emphasizes the critical importance of optimized additive ratios, and demonstrates the potential of predictive models for preliminary design in sustainable soil stabilization.

1. INTRODUCTION

Clay soils, particularly those dominated by aluminosilicate minerals, are known for their high plasticity, low shear strength, and poor compaction capability, making them unsuitable for foundations and pavement subgrades in their natural state (Noaman *et al.,* 2020). Traditional stabilizers such as cement and lime have been widely used to overcome these limitations; however, their high carbon footprint and increasing costs have prompted researchers to explore sustainable alternatives (Singh and Kumar, 2022). Agro-waste and industrial by-products, including millet husk ash (MHA), quarry dust (QD), and bush gravel (BG), have shown significant potential as stabilizing agents due to their favorable chemical and physical characteristics.

MHA contains high quantities of amorphous silica capable of reacting with calcium to form cementitious calcium–silicate–hydrate (C–S–H) gels, aligning with standard pozzolanic behaviour described in ASTM C618 (2019). Quarry dust not only supplies essential calcium for pozzolanic activation but also acts as a micro-filler that enhances soil packing and reduces void ratios (Zhang *et al.,* 2021). Bush gravel, being a granular material, provides mechanical reinforcement through particle interlock and friction, thereby improving stress transfer, enhancing load distribution, and reducing deformation in weak soils (Zaini *et al.,* 2024). revious studies have shown that combined chemical and physical stabilization can greatly improve the engineering properties of weak soils (Nnochiri *et al.,* 2022).

This study evaluates the stabilization of clay soil using optimized proportions of MHA, QD, and BG. It integrates experimental geotechnical tests, microstructural characterization, and predictive modelling of unconfined compressive strength (UCS). The modelling component is designed to support pavement design and soil classification frameworks such as those outlined in AASHTO M 145 (1991).

2. MATERIALS AND METHODS

2.1 Materials and Equipment

The materials used in this research include clay soil, millet husk ash (MHA), quarry dust (QD), and bush gravel (BG). The native clay soil was collected from Deeper Life Camp, Aviele, located in Etsako West Local Government Area of Edo State, along the Benin–Auchi Expressway. This clay soil is naturally high in plasticity, with low shear strength and poor compaction characteristics, making stabilization necessary for engineering applications. Millet husk ash (MHA) was produced through controlled combustion of millet husks at a temperature range of 600–650 °C. This ensured complete carbonization, producing a fine, pozzolanic ash suitable for enhancing clay soil properties.

Quarry dust (QD) was obtained from a local quarry in Uloke, Etsako West, along the Benin–Abuja Expressway. Its fine mineral particles improve the mechanical properties of clay soil by reducing plasticity and enhancing shear strength. Bush gravel (BG) was collected from open fields in Fugar, Etsako Central Local Government Area, where it is abundant. The coarse nature of BG provides mechanical interlocking, improving load-bearing capacity when combined with other stabilizers. All materials were stored in dry (Figure 1) conditions prior to preparation to prevent moisture variability

Figure 1: Packed Materials for Laboratory Analysis

2.2 Sample Preparation

a. Soil Samples

The soil samples were air-dried, pulverized, and sieved sequentially through mechanical sieves (Figure 2.2) of sizes 20 mm, 10 mm, 4.75 mm, 2 mm, and 0.425 mm to ensure uniform particle distribution. This preparation was carried out at the Civil Engineering Soil Laboratory, Edo University Iyamoh.

Figure 2: Mechanical Sieving of Materials

b. Millet Husk Ash.

The millet was collected and burnt under a controlled temperature in an open furnace (Figure 3) producing ash (Figure 4) used for the analysis.

Figure 3: Burning of Millet to Ash

Figure 4: Millet Husk Ash

Millet husk ash was initially passed through a full range of sieves (20 mm, 10 mm, 4.75 mm, 2.00 mm, and 0.425 mm), only the **2.00 mm and 0.425 mm sieves were finally adopted** for the preparation of MHA used in the experimental program. This was intentional and technically justified because MHA was used as a **pozzolanic binder,** only fine particles passing 2.00 mm and 0.425 mm were retained to ensure maximum reactivity, uniform mixing, and effective void filling, while coarser unreactive residues were discarded.

c. Quarry Dust

The quarry dust was air-dried to remove moisture and manually crushed to eliminate lumps. It was initially screened using a full range of sieves of sizes 20 mm, 10 mm, 4.75 mm, 2.00 mm, and 0.425 mm to remove oversized particles and ensure grading control. However, only particles passing the 4.75 mm sieve were finally retained for use in the experiments, while coarser fractions were discarded. This maximum particle size was selected to allow quarry dust to act as a fine aggregate and void-filling stabilizer, improving particle packing within the clay matrix.

d. Bush Gravel

Bush gravel was washed, air-dried, and manually broken to remove oversized lumps. It was then initially sieved through a full set of sieves of sizes 20 mm, 10 mm, 4.75 mm, 2.00 mm, and 0.425 mm to separate different size fractions. However, only particles retained between 4.75 mm and 20 mm were finally used in the experiments, while finer materials passing the 4.75 mm sieve were discarded. This size range was selected to preserve the role of bush gravel as a coarse reinforcing agent, providing mechanical interlocking, improved load transfer, and structural stability within the stabilized soil mass.

e. Design of Experiment (DOE) and Sample Preparation.

A Design of Experiment (DOE) approach using the Taguchi method in Minitab software was employed to determine the optimal mix proportions for the study. The factors and level used for the DOE approach is shown in Table 1.

Table 1: Factors and Levels for DOE

Factors	Levels
MHA	5, 10, 15
BG	10, 15, 20
QD	20, 25, 30

The DOE employed three control factors Millet Husk Ash (MHA), Quarry Dust (QD), and Bush Gravel (BG) each at three levels to capture their individual and combined effects on soil stabilization. These factor levels were selected based on preliminary tests and literature to ensure meaningful performance variation across the experimental runs. Minitab generated the design matrix showing the experimental runs as shown in Table 2 used for the treatment of the clay soil.

Table 2: Runs Obtained from DOE

S/no	MHA	QD	BG
1.	5	10	20
2.	5	15	25
3.	5	20	30
4.	10	10	25
5.	10	15	30
6.	10	20	20
7.	15	10	30
8.	15	15	20
9.	15	20	25

The Taguchi DOE allowed for systematic variation of these additives while minimizing the number of experimental trials, ensuring efficient exploration of the effects of each stabilizer on the clay soil properties. Based on the DOE results, the clay soil samples were carefully mixed with the varying quantities of additives. The exact amounts of each additive were calculated using the formula:

$$Weight\ of\ additive = \frac{100\ g\ \times weight\ of\ additive\ (\%)}{100} \tag{1}$$

The soil and additives were carefully weighed and gradually mixed to ensure uniform distribution to obtain the different mix proportion for stabilization as shown in Table 3.

Water was then added to achieve the optimum moisture content, and the mixtures were thoroughly kneaded to ensure homogeneity. Each mixture was compacted using the Standard Proctor compaction method (ASTM D698, 2012). The compacted specimens (Figure 5) were extruded from the molds and sealed in airtight polyethylene bags to prevent moisture loss. Samples were cured for seven days at controlled room temperature (23–25 °C) to allow pozzolanic reactions and particle restructuring, as recommended in previous studies (Noaman *et al.,* 2020).

Table 3: Different Mix Proportion for Stabilization

Runs	MHA (g)	QD (g)	BG (g)
1	50	100	200
2	50	150	250
3	50	200	300
4	100	100	250
5	100	150	300
6	100	200	200
7	150	100	300
8	150	150	200
9	150	200	250

Figure 5: Compacted Soil Samples

f. Microstructural Analysis

Microstructural examination was carried out using scanning electron microscopy with energy dispersive X-ray spectroscopy (SEM–EDX) at Nigerian Building & Road Research Institute (NIBRRI) Abuja, Nigeria. This allowed visualization of soil morphology, identification of bonding phases such as C–S–H, and assessment of the elemental composition responsible for chemical reactions.

g. UCS and CBR Test

Unconfined compressive strength tests were performed on cylindrical specimens (Figure 2.5) following ASTM D2166/D2166M (2016). Each sample was axially loaded at a constant strain rate until failure, and the maximum axial stress was recorded as the UCS. California Bearing Ratio tests were conducted in accordance with AASHTO T193, where soaked samples were subjected to penetration loading at standard rates. Compaction characteristics, including MDD and OMC, were determined following the procedures in ASTM D698 (2012).

h. Modelling

Predictive modelling focused on estimating UCS based on the proportions of MHA, QD, and BG. Four machine learning techniques were employed: Linear Regression, Gaussian Process Regression (GPR), Support Vector Regression (SVR) with RBF kernel, and Bayesian Ridge Regression. Model performance was quantified using mean absolute error (MAE), root mean square error (RMSE), and coefficient of determination (R^2). The approach aligns with recent applications of machine learning in geotechnical engineering (Zhang *et al.,* 2021).

3. RESULTS AND DISCUSSION

3.1 Experimental Results

The incorporation of millet husk ash (MHA), quarry dust (QD), and bush gravel (BG) markedly improved the geotechnical properties of the clay soil. The results for unconfined compressive strength (UCS) (Table 4 and Figure 6), California Bearing Ratio (CBR), maximum dry density (MDD) (Table 5 and Figure 7), and optimum moisture content (OMC). These parameters provide a clear indication of the soil's suitability for subgrade and sub-base applications.

Table 4: UCS Values for Treated and Untreated Clay Soil

Samples	**Mix Design**			**Experimental**
	MHA	**BG**	**QD**	**UCS kPa)**
Untreated Soil	0	0	0	289
1	5	10	20	1295
2	5	15	25	1459
3	5	20	30	1063
4	10	10	25	1098
5	10	15	30	1315
6	10	20	20	819
7	15	10	30	1003
8	15	15	20	401
9	15	20	25	803

Table 3.1 shows that the inclusion of MHA, BG and QD significantly increased UCS compared to the untreated soil (289 kPa), as determined using **ASTM D2166/D2166M.** The highest strength (1459 kPa) was achieved at **5% MHA, 15% BG and 25% QD,** indicating an optimum blend, while excessive stabilizer contents (Sample 8) caused strength reduction, confirming that performance depends on proper proportioning rather than quantity alone. Figure 6 graphically presents the UCS results for the treated and untreated soil samples. From the chart, it is observed that **all stabilized mixes recorded significantly higher UCS values than the untreated soil (289 kPa), indicating the effectiveness of MHA, BG and QD in improving soil strength.**

The maximum UCS (1459 kPa) occurred at Sample 2 (5% MHA, 15% BG, 25% QD), showing an optimum stabilizer combination, while excessive additive content led to strength reduction in some mixes as shown in sample 8.

Table 5 presents the OMC, MDD and CBR results obtained in accordance with **ASTM D698** and **AASHTO T193.** The results show that stabilization increased OMC and generally improved MDD and CBR relative to untreated soil, indicating better compaction behaviour and strength. Samples 2 and 3 recorded the highest CBR values (>13%), reflecting superior load-bearing capacity. In contrast, excessive stabilizer content (Sample 8) caused reduced density and lower CBR, confirming the need for optimum proportioning.

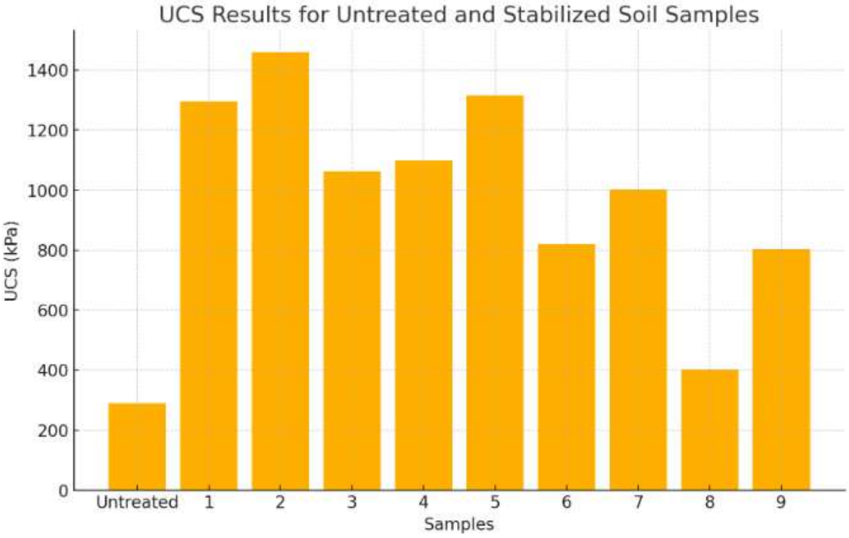

Figure 6: UCS values for Treated and Untreated Soil Samples

Table 5: Geotechnical Properties of Stabilized Soil

Samples	OMC (%)	MDD (g/cm^3)	CBR (%)
Untreated Soil	13.1	1.62	4.2
1	18.66	1.66	9.5
2	19.42	1.74	13.2
3	19.64	1.74	13.5
4	26.11	1.65	8.7
5	21.10	1.72	12.1
6	19.46	1.65	10.4
7	20.81	1.63	7.6
8	24.54	1.49	6.8
9	22.27	1.51	7.4

Figure 7 shows the combined effect of stabilization on compaction and strength parameters. The treated samples generally exhibit higher OMC and improved MDD compared to untreated soil, indicating better moisture demand and packing characteristics.

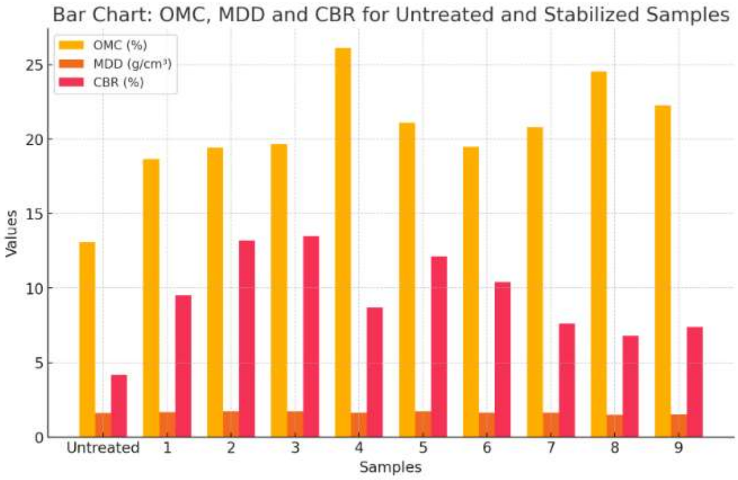

Figure 7. Comparison of OMC, MDD & CBR of Treated and Untreated Soil

Samples 2 and 3 recorded the highest CBR values, corresponding with relatively high MDD as determined using **ASTM D698,** indicating improved compaction characteristics and load-bearing capacity in accordance with **AASHTO T193.** In contrast, lower performance in Sample 8 confirms that excessive stabilizer content reduces dry density and strength, thereby limiting suitability as a pavement subgrade material under standard specifications.

3.2 Microstructural Analysis

The mineral composition of the soil and additives (Figure 8) played a central role in the behaviour of the stabilized mixtures. The natural clay (Sample A) was dominated by alumino-silicate minerals, which explained its low inherent engineering performance, reflected in an initial UCS of **289 kPa,** CBR of **4.2%,** MDD of **1.62 g/cm³,** and OMC of **13.1%.** Millet husk ash contained a high proportion of reactive silica (**23.91 wt%)** and oxygen (**54.29 wt%),** which is consistent with the pozzolanic characteristics of agricultural bio-ashes reported by Nnochiri *et al.,* (2022). Quarry dust derived from granite contributed additional silica (**16.96 wt%)** and calcium (**6.10 wt%),** providing essential mineral components for initiating and sustaining pozzolanic bonding, as outlined by Zhang *et al.,* (2021). Bush gravel, with approximately **24.50 wt% silica,** mainly served as a mechanical stabilizer by forming a granular skeleton that improved particle interlock and load transfer.

(A) **(B)** **(C)**

Figure 8: Micrograph of Untreated Soil (A) and Treated Soil Samples (N1-N9) represented with (B & C)

Compared with the natural clay soil, which contained O = 54.40 wt%, Si = 19.35 wt%, Al = 12.00 wt%, and no detectable calcium, the treated samples (N1–N9) exhibited clear chemical transformation due to the combined effects of millet husk ash, quarry dust, and bush gravel. Oxygen levels generally increased to about 51–60 wt%, while silica content increased in several mixtures, reaching a maximum of 30.87 wt% in N6, confirming strong enrichment from the additives. Alumina and iron contents decreased markedly in many treated samples (for example, Al = 4.26 wt% in N5 and very low Fe levels in N2–N7), indicating reduced clay reactivity. Calcium, which was absent in the natural soil, appeared in treated mixes (for example, 1.76 wt% in N5 and 1.09 wt% in N6), validating the contribution of quarry dust and the formation of cementitious compounds. The increase in carbon content in some samples (for example, 19.91 wt% in N5) further reflects the organic influence of millet husk ash (11.93 wt% C).

Overall, these changes (Figure 8 (B & C) demonstrate that the soil system transitioned from a weak alumino-silicate structure to a stabilized matrix characterized by increased silica availability, calcium activation, and reduced clay activity. This chemical transformation directly accounts for the observed improvements in strength, compactability, and overall stability as the treatment percentages increased.

3.3 Predictive Modelling Performance

SVR used the RBF kernel with parameters **C, γ**, and **ε**, optimized via cross-validation, while GPR used an **RBF (squared exponential) kernel** with a white-noise term, with hyperparameters **$\sigma^2 f$, ℓ,** and **$\sigma^2 n$** estimated by maximizing the log-marginal likelihood. Table 6 presents the descriptive statistics of the experimental dataset used for predictive modelling. The dataset comprises **9 unique experimental mixtures** generated from a Taguchi L9 orthogonal array. Each mixture contained measured proportions of MHA, QD and BG, with corresponding UCS outcomes.

Table 6. Statistical Dataset of Variables

Variable	Count	Mean	Std	Min	25%	50%	75%	Max
MHA	9.0	10.000	4.330	5.0	5.0	10.0	15.0	15.0
QD	9.0	15.000	4.330	10.0	10.0	15.0	20.0	20.0
BG	9.0	25.000	4.330	20.0	20.0	25.0	30.0	30.0
UCS	9.0	1028.444	4.330	401.0	819.0	1063.0	1295.0	1459.0

This distribution reflects controlled variation across stabilization components with a wide response range in UCS, making it suitable for comparative model evaluation despite limited sample size. Four predictive models were evaluated: **Linear Regression, Gaussian Process Regression (GPR), Support Vector Regression (SVR) with RBF kernel, and Bayesian Ridge Regression.** Model accuracy was assessed using **MAE, RMSE and R^2** as shown in Table 7.

Table 7. Predictive Model Performance

Mix Ratio MHA, QD, BG	MAE (kPa)	RMSE	R2
Linear Regression	227.03	296.09	-0.132
GPR	209.24	295.76	0.056
SVR (RBF)	259.95	323.87	-0.087
Bayesian Ridge	230.57	306.85	-0.104

Due to the limited dataset size **(n = 9 experimental mixtures),** all predictive models were evaluated using internal validation. Support Vector Regression (SVR) was implemented using a **Radial Basis Function (RBF) kernel** with default regularization and kernel parameters (C and γ). Gaussian Process Regression (GPR) employed a **squared-exponential (RBF) covariance kernel,** with hyperparameters (length scale and signal variance) optimized using maximum likelihood estimation. Linear Regression and Bayesian Ridge were included as baseline linear models for comparison.

Among the four models evaluated, **GPR demonstrated the strongest predictive performance,** producing the lowest MAE (209.24 kPa) and RMSE (295.76 kPa), and the only positive R^2 value (0.056). This indicates that GPR was the only model capable of capturing part of the **nonlinear relationship between MHA–QD–BG proportions and UCS development.**

Linear Regression recorded higher error values (MAE = 227.03 kPa; RMSE = 296.09 kPa) and a negative R^2 (–0.132), confirming that linear assumptions were inadequate for modeling the complex mechanical and chemical interactions occurring in the stabilized soil. Similarly, **SVR performed poorly** (MAE = 259.95 kPa; RMSE = 323.87 kPa; R^2 = –0.087), which is attributed mainly to insufficient data for effective kernel parameter optimization.

Bayesian Ridge also exhibited limited predictive capability (MAE = 230.57 kPa; RMSE = 306.85 kPa; R^2 = –0.104), indicating that even with regularization, linear-based approaches were unable to account for nonlinear strength contributions arising from pozzolanic reactions and granular reinforcement mechanisms.

4. CONCLUSION

This study demonstrated that millet husk ash (MHA), quarry dust (QD) and bush gravel (BG) significantly improve the engineering behaviour of weak clay soils. The optimum blend of **5% MHA, 15% QD and 25% BG** achieved a UCS of **1459 kPa,** representing over a fourfold increase compared to the untreated soil, alongside notable improvements in **CBR, MDD and compaction efficiency.** SEM–EDX analysis confirmed improved microstructural bonding through denser particle packing and the formation of **C–S–H gels,** resulting from reactive silica in MHA, calcium contributions from QD, and mechanical interlocking provided by BG.

Predictive modelling revealed that strength development in stabilized soils is strongly **nonlinear,** with **Gaussian Process Regression (GPR)** outperforming Linear Regression, SVR and Bayesian Ridge (MAE = 209.24 kPa, RMSE = 295.76 kPa, $R^2 = 0.056$). Overall, **GPR emerged as the most reliable model,** while the remaining approaches were constrained by small dataset size and limited ability to represent nonlinear soil–stabilizer interactions. These findings highlight the suitability of **kernel-based machine learning techniques** for modelling stabilized soils and emphasize the need for **larger datasets** to improve prediction accuracy and reliability in geotechnical applications. Collectively, the results confirm that MHA, QD and BG offer a **cost-effective and sustainable solution** for subgrade and sub-base stabilization.

5. RECOMMENDATIONS

The following recommendations are proposed based on the findings of this study to improve the application of MHA, QD and BG in soil stabilization and to guide future research. They are intended to enhance performance reliability and predictive accuracy in practical engineering applications. The recommendations include;

1. The 5% MHA + 15% QD + 25% BG mix is recommended for practical stabilization.
2. MHA should be limited to ≤10% to avoid strength reduction.
3. Future studies should include extended curing periods and additional variables (mineralogy, PSD, temperature) to improve modelling accuracy.
4. Field trials and durability tests (wet–dry, freeze–thaw, sulphate resistance) are recommended to validate long-term performance.
5. Life-cycle and economic assessments should be conducted to support large-scale adoption.

Abbreviations

QD	Quarry Dust
BG	Bush Gravel
MHA	Millet Husk Ash
PSD	Heating, Ventilation, and Air Conditioning
CBR	California bearing ratio
MDD	Maximum dry density
OMC	Optimum moisture content
UCS	Unconfined comprehensive strength
SEM	Scanning Electron Microscope
EDX	Energy Dispersive X-ray
MAE	Mean absolute error
RMSE	Root mean square error
R^2	Coefficient of determination
GPR	Gaussian Process Regression
SVR	Support Vector Regression
kPa	**kilopascal**

ACKNOWLEDGEMENTS

The authors acknowledge the Faculty of Engineering, Edo State University, Iyamho for providing laboratory facilities and technical support. Special appreciation goes to Prof Wasiu, Dr. Kennedy Adama, Engr. Mrs Parker Ikharo-F and Engr Adoga E. A for their valuable contributions to this research.

REFERENCES

AASHTO M 145 (1991). *Classification of Soils and Soil-Aggregate Mixtures for Highway Construction.* American Association of State Highway and Transportation Officials.

AASHTO T193. *Standard Method of Test for the California Bearing Ratio.*

ASTM C618 (2019). *Standard Specification for Coal Fly Ash and Raw or Calcined Natural Pozzolan for Use in Concrete.*

ASTM International. ASTM D2166/D2166M (2016). *Standard Test Method for Unconfined Compressive Strength of Cohesive Soil.* ASTM International.

ASTM International. ASTM D698 (2012). *Standard Test Methods for Laboratory Compaction Characteristics of Soil Using Standard Effort.* ASTM International.

Nnochiri, E. S., Edeh, J. E., & Moses, G. (2022). Bio-ash stabilization of clay soils. *International Journal of Geotechnical Engineering*, 16(4), 321–334.

Noaman, H., Ahmed, S., & Karim, M. (2020). *Engineering properties of stabilized clay soils*. Journal of Civil Engineering Research, 5(2), 45–58.

Singh, R., & Kumar, A. (2022). Sustainable Clay Stabilization Techniques: Chemical and Physical Interactions. *Advances in Civil Engineering*, 2022, 1–15.

TRRL Road Note 31 (1977). *Strength Criteria for Pavement Materials.* Transport and Road Research Laboratory, UK.

Zaini, M. S. I., Hasan, M., & Almuaythir, S. (2024). *Experimental study on the use of polyoxymethylene plastic waste as a granular column to improve the strength of soft clay soil.* **Scientific Reports, 14,** 22558.

Zhang, P., Yin, Z.-Y., & Jin, Y.-F. (2021). State-of-the-art review of machine learning applications in constitutive modelling of soils. *Archives of Computational Methods in Engineering*, 28(5), 3661–3686.